Taylor & Francis
Taylor & Francis Group

Check for updates

ORIGINAL RESEARCH

CYTL1 inhibits tumor metastasis with decreasing STAT3 phosphorylation

Xiaolin Wang[a,b], Ting Li[a], Yingying Cheng[a,c], Pingzhang Wang[a], Wanqiong Yuan[a], Qiyao Liu[a], Fan Yang[d], Qiang Liu[d], Dalong Ma[a], Shigang Ding[e], Jun Wang[d], and Wenling Han[a]

[a]Peking University Center for Human Disease Genomics, Department of Immunology, Key Laboratory of Medical Immunology, Ministry of Health, School of Basic Medical Sciences, Peking University Health Science Center, Beijing, China; [b]Laboratory of Immunology, Beijing Pediatric Research Institute, Beijing Children's Hospital, Capital Medical University, National Center for Children's Health, Beijing, China; [c]Department of Laboratory Medicine, Affiliated Hospital of Nanjing University of Traditional Chinese Medicine, Nanjing, Jiangsu, China; [d]Department of Thoracic Surgery, Peking University People's Hospital, Beijing, China; [e]Department of Gastroenterology, Peking University Third Hospital, Beijing, China

ABSTRACT

CYTL1 is a novel cytokine that was first identified in CD34^{+} hematopoietic cells. We previously prepared recombinant CYTL1 and verified that it chemoattracted human monocytes via the CCR2/ERK pathway. It has been reported that CYTL1 plays contradictory roles in neuroblastoma and lung cancer. We found that the expression level of CYTL1 was notably decreased and it was hypermethylated in various tumors, including breast and lung cancer, by bioinformatics analyses. After validating the expression of CYTL1 in lung cancer, we identified that CYTL1 exerted no obvious effect on tumor cell proliferation but inhibited their migration and invasion, and these effects were accompanied by decreasing STAT3 phosphorylation, using recombinant CYTL1 and CYTL1-overexpressing tumor cell lines. Furthermore, we constructed experimental and spontaneous metastasis models of breast cancer in BALB/c mice and found that CYTL1 significantly inhibited tumor metastasis *in vivo*. In summary, CYTL1 is a cytokine with tumor-suppressing characteristics that inhibits tumor metastasis and STAT3 phosphorylation in multiple types of tumors.

Introduction

Cytokine-like 1 (CYTL1, also known as C17 or C4ORF4) is a secreted protein with 136 amino acids that was first identified in human CD34^{+} hematopoietic cells.[1] CYTL1 is abundantly expressed in cartilaginous tissues, including the mouse inner ear and human articular cartilage,[2,3] and thus contributes to cartilage homeostasis and the inhibition of osteoarthritic cartilage destruction.[4,5] A previous study demonstrated that CYTL1 prevents inflammatory arthritis and significantly downregulates the expression of inflammatory cytokines.[6] It appears that CYTL1 performs anti-inflammatory functions, but the mechanism remains unknown. To obtain recombinant CYTL1 protein for functional studies, we established a stable expression system and obtained high-quality CYTL1. In addition, we demonstrated that replacement of the native signal peptide of CYTL1 with the Igκ signal peptide increased the expression and secretion of CYTL1.[7] The chemokine receptor CCR2 was proposed to be a potential receptor of CYTL1 based on the hypothesis that CYTL1 could be a structural and functional analog of CCL2 signaling.[8] Using the purified protein, we verified that CYTL1 chemoattracts human monocytes via the CCR2/ERK pathway.[9]

It has also been reported that CYTL1 is highly expressed in the neuroblastoma cell line SH-SY5Y, and the knockdown of CYTL1 with siRNA inhibits the proliferation, migration and

invasion of neuroblastoma cells.[10] Moreover, *CYTL1* is hypermethylated and downregulated in human lung squamous cell carcinomas (SCCs). DNA methylation is related to the gene expression at the very early stage of tumorigenesis and methylation at the promoter region leads to gene silencing. Downregulation of CYTL1 in SCCs is consistent with its hypermethylation.[11] The above-mentioned studies suggest that the cytokine CYTL1 shows different expression patterns and functions in different types of tumors.

Mounting evidence suggests important regulatory roles for cytokines in carcinogenesis beyond their key functions in immune responses and inflammation.[12] Notably, different types of cytokines perform a broad spectrum of tumor-suppressing functions. For instance, IL-24 has been proven to suppress multiple signaling pathways in various human cancer cells, such as melanoma, cervical cancer, lung cancer and prostate cancer,[13] and this suppressive effect leads to tumor cell death and the inhibition of tumor angiogenesis and metastasis.[14,15] Because recombinant IL-24 shows selective cytotoxicity against cancer cells, clinical trials have investigated the use of IL-24 for the treatment of solid tumors.[16,17] Another example is IL-37, whose intracellular mature form markedly inhibits the migration of multiple types of tumor cells by inhibiting Rac1 activation.[18] Moreover, certain cytokines, such as IL-6, exert tumor-promoting effects. In the tumor microenvironment, IL-6/

CONTACT Shigang Ding ✉ dingshigang222@163.com 🖃 Department of Gastroenterology, Peking University Third Hospital, Beijing 100191, China; Jun Wang jwangmd@yahoo.com 🖃 Department of Thoracic Surgery, Peking University People's Hospital, 11 Xi-Zhi-Men South Street, Beijing 100044, China; Wenling Han hanwl@bjmu.edu.cn 🖃 Peking University Center for Human Disease Genomics, Department of Immunology, Key Laboratory of Medical Immunology, Ministry of Health, School of Basic Medical Sciences, Peking University Health Science Center, 38 Xueyuan Road, Beijing 100191, China
🅑 Supplemental data for this article can be accessed on the publisher's website.

STAT3 signaling performs strong promoting functions in the growth and development of many human cancers, including lung cancer and breast cancer, while suppressing the anti-tumor immune response.[19] Preclinical studies have suggested that the anti-IL-6R antibody tocilizumab is effective against ovarian[20] and pancreatic cancer.[21] The safety and effectiveness of tocilizumab in patients with B cell chronic lymphocytic leukemia and in those with breast or pancreatic cancers have been evaluated in early phase trials.[19] Clinical evaluations have shown that the STAT3 antisense oligonucleotide AZD9150 possesses activity against treatment-refractory lymphoma and lung cancer.[22] C188-9, another high-affinity STAT3 inhibitor, is currently being evaluated in a phase I study involving patients with advanced-stage solid tumors.[23] Therefore, the identification of novel cytokines associated with tumor development and metastasis could be important for prognosis and treatment.

We found a notable downregulation of CYTL1 in most types of tumors, including breast, prostate, lung and stomach cancer, by an integrated bioinformatics analysis. However, CYTL1 expression was unchanged or upregulated in some other tumors, such as thyroid carcinoma and kidney renal clear cell carcinoma. Our analysis also revealed CYTL1 hypermethylation and downregulation of CYTL1 expression in various types of tumors. The results of the bioinformatics analysis suggested that CYTL1 might play important roles in tumor progression and development.

We mainly focused on the function of CYTL1 in tumors with decreased CYTL1 expression. First, we experimentally validated the downregulation of CYTL1 in lung cancer, and then, we explored the effects of this cytokine on the proliferation and migration of the lung cancer cell line A549 and several other tumor cell lines, including the breast cancer cell line MDA-MB-231 and the prostate cancer cell line PC3. The results showed that CYTL1 exerted broad-spectrum inhibitory impacts on tumor cell migration and invasion and on the phosphorylation of STAT3. These effects were further verified *in vivo* using experimental and spontaneous metastasis models of breast cancer in BALB/c mice. In summary, we demonstrated that CYTL1 exhibits tumor-suppressing characteristics in multiple types of carcinomas through inhibitory effects on metastasis and STAT3 phosphorylation.

Materials and methods

Bioinformatics

All array data related to cancers from the Affymetrix human genome U133 plus 2.0 platform were downloaded from the Gene Expression Omnibus (GEO) (http://www.ncbi.nlm.nih.gov/geo/) and the Cancer Genome Atlas (TCGA) databases (https://cancergenome.nih.gov/). The expression profile and methylation of CYTL1 in multiple types of cancers and corresponding control (normal or non-tumor) tissues were evaluated, and the expression levels and beta values are presented in box plots.

Patient samples

A total of 60 patients with lung cancer who underwent surgery at Peking University People's Hospital (Beijing, China) were enrolled in the present study. Paired tumor and adjacent non-tumor tissues were collected, and CYTL1 expression was assessed. All the specimens were pathologically confirmed. All participants provided informed consent according to the Helsinki Declaration, and the protocol used in the present study was approved by the Ethics Committee of Peking University People's Hospital (Beijing, China).

Cell lines

The following cancer cell lines were used in this study: three lung cancer cell lines (A549 cells, PC9 cells and Lewis lung carcinoma cells (LLC1)) and the breast cancer cell line (MDA-MB-231 cells) were maintained in our laboratory; the prostate cancer cell line (PC3 cells) was obtained from the Department of Urology at Peking University People's Hospital (Beijing, China); and the breast cancer cell line (4T1-luc cells) stably expressing luciferase was provided by Prof. Wang Yu from Tianjin Medical University. The A549, PC9, PC3 and MDA-MB-231 cells were cultured routinely in RPMI1640 (HyClone, Logan, UT, USA) containing 10% fetal bovine serum (FBS; HyClone) supplemented with 1% penicillin/streptomycin. The LLC1 and 4T1-luc cells were cultured routinely in DMEM (HyClone) containing 10% FBS (HyClone) supplemented with 1% penicillin/streptomycin. All the cells were grown at 37°C in a humidified incubator containing 5 % CO_2.

Transfection and infection

The expression vectors pcDNA3.1-CYTL1-his, TG006-Native-CYTL1, TG006-Igκ-CYTL1 and pLenti6.3/V5-Topo-Cytl1 were constructed. pcDNA3.1-CYTL1-his, TG006-Native-CYTL1 and TG006-Igκ-CYTL1 contain the human *CYTL1* gene, and pLenti6.3/V5-Topo-Cytl1 contains the mouse *Cytl1* gene. The lentiviral vector TG006 contains GFP, and pLenti6.3/V5-Topo contains the blasticidin resistance fusion gene. The pcDNA3.1-CYTL1-his plasmid was transfected into A549 cells using VigoFect (Vigorous, Beijing, China) according to the manufacturer's instructions. The culture medium was replaced 8 h post-transfection with Hektor's medium (Cell Culture Technologies, Zurich, Switzerland) supplemented with 2% glutamate (Sigma-Aldrich, St. Louis, MO, USA). The cell lysate and supernatant were harvested 48 h after medium replacement. Lentiviral particles were produced by transfecting HEK293T cells with either (1) TG006-Native-CYTL1, TG006-Igκ-CYTL1 or empty TG006 vector along with the psPAX2 and pMD2.G packaging vectors or (2) pLenti6.3/V5-Topo-Cytl1 vector or empty pLenti6.3/V5-Topo vector along with the psPAX2 and pCMV-VSV-G packaging vectors. Supernatants containing the lentiviral particles were harvested 48 h after transfection. The packaging vectors were purchased from Thermo Fisher Scientific (Waltham, MA, USA). A549 cells were infected with the TG006-Native-CYTL1 or TG006-Igκ-CYTL1 lentiviral particles, and cells stably infected with the

expression vector containing GFP were acquired through cell sorting by FACS. A549 cells stably expressing CYTL1 were designated A549-Native-CYTL1 and A549-Igκ-CYTL1, and the control cells were designated A549-TG006. The 4T1-luc cells were infected with the pLenti6.3/V5-Topo-Cytl1 lentiviral particles and then subjected to 4 μg/ml blasticidin (Univ-Bio Company, Shanghai, China) selection for 14 days. 4T1-luc-Cytl 1 cells were then constructed, and the control cells were designated 4T1-luc-Topo.

Protein extraction and western blotting

The cells were lysed in RIPA buffer (Sigma-Aldrich) containing 1% protease inhibitor cocktail and 1% PhosSTOP (Roche, Basel, Switzerland). The protein concentrations were determined through BCA protein assays (Pierce, Rockford, IL, USA), and the whole cell lysates were fractionated by 12.5% SDS-PAGE and electrotransferred onto polyvinylidene difluoride membranes (Hybond, GE Healthcare, Buckinghamshire, UK). Western blotting was performed as previously described. Rabbit anti-CYTL1 polyclonal antibody was prepared in our laboratory, and antibodies against t-STAT3, p-STAT3 (Y705), t-Akt, p-Akr, t-ERK, p-ERK, t-p65 and p-p65 were purchased from Cell Signaling Technology (Danvers, MA, USA). Anti-β-actin antibody was purchased from Sigma-Aldrich, and β-actin blotting was used as a lysate loading control. The densities of the bands were analyzed using ImageJ software (National Institutes of Health, Bethesda, MD, USA) and normalized to those of β-actin.

PCR and qPCR

Total RNA from lung cancer tissues and cell lines was isolated using TRIzol reagent (Invitrogen, Carlsbad, CA, USA). Reverse transcription was performed according to standard protocols using a RevertAid™ II First-strand cDNA synthesis Kit (Thermo Fisher Scientific Inc., Waltham, MA, USA). Semiquantitative PCR and qPCR (quantitative PCR) were performed as previously described.[7,24] GAPDH was amplified as an internal standard. The following primers were used for the PCR of CYTL1: CYTL1-F, 5′-ATCACCCGCGACTTCAAC-3′; and CYTL1-R, 5′-CAGCTTGTCCAGCACACAGT-3′.

Cell proliferation assay

Cell proliferation was measured using a Cell Counting Kit-8 (CCK8) detection kit (Dojindo Molecular Technologies, Japan). WST-8 [2-(2-methoxy-4-nitrophenyl)-3-(4-nitrophenyl)-5-(2,4- disulfophenyl)-2H-tetrazolium, monosodium salt] in reagent produces a water-soluble formazan dye upon reduction by dehydrogenase in mitochondria in the presence of an electron mediator. The amount of formazan dye is directly proportional to cell number. The cells were seeded at a concentration of 1500 cells per well in a 96-well plate and either treated with recombinant human CYTL1 protein (1, 10, 100, and 1000 ng/ml)[7] or not treated. At the indicated time points, 10 μl of CCK-8 solution was added to each well, and the plate was then incubated at 37°C for 100 min. The absorbance values of all the wells at 450 nm were subsequently determined.

Wound-healing assay

Wound-healing assay is performed to detect the migration rate of tumor cells. The cells were seeded in a six-well plate, grown to 80% confluence and then treated or not treated with 100 ng/ml recombinant human CYTL1 protein. In the middle of the cell monolayer, a wound was carefully scrapped with a sterilized pipette tip. Photomicrographs were taken 48 h after scrapping. The wound widths in the microscopic pictures were measured at different time points using ImageJ software. The percentage of wound healing was calculated based on the initial wound width at 0 h.

Cell migration and invasion assay

Cell migration and invasion were analyzed using Transwell chambers (8-μm pore size, BD Biosciences, NJ, USA). The cells were cultured in serum-free RPMI1640 medium for 16 h and then seeded into the upper chamber at a density of 5×10^4 cells per well in 0.25 ml of serum-free RPMI1640 medium with or without 100 ng/ml recombinant human CYTL1 protein (100 ng/ml recombinant mouse CYTL1 protein for LLC1 cells[9]). The upper chamber was pre-coated with (for the invasion assay to assess tumor cell invasion) or without (for the Transwell assay to assess tumor cell migration) Matrigel, and 0.5 ml of RPMI-1640 with 10% FBS was added to the lower chamber. After incubation at 37°C in an atmosphere with 5% CO_2 for 24 h (for the Transwell assay) or 48 h (for the invasion assay), the chambers were disassembled, and the membranes were fixed in 4% paraformaldehyde/PBS for 10 min and stained with 2% crystal violet for 10 min. The number of cells was counted, and images were obtained under a microscope (100 × magnification) (IX73, Olympus, Tokyo, Japan).

Breast cancer experimental metastasis model

Five- to six-week-old female BALB/c mice were purchased from Vital River (Beijing, China). The mice were bred and maintained under specific pathogen-free conditions, provided sterilized food and water and housed in a barrier facility under a 12-h light/dark cycle. The mice were randomly divided into two groups and injected with 4T1-luc-Topo cells or 4T1-luc-Cytl1 cells (n = 4). In total, 1×10^6 cells in 200 μl of PBS were injected through the vena caudalis into each mouse. After 9 days, D-luciferin (PerkinElmer, USA) was injected into the abdominal cavity of the mice, and 12 min after the injection, tumor growth and metastasis were monitored in vivo via fluorescence intensity measurements using the IVIS Spectrum Imaging System (PerkinElmer). All the mice were sacrificed on day 9, and the lungs were removed. After staining with Bouin's solution for 24 h, the lungs were cut into blocks and embedded in paraffin for H&E staining. To monitor the survival rate, 13 additional mice in each group were used to construct the breast cancer experimental metastasis model, and these mice were bred and maintained for 40 days.

Breast cancer spontaneous metastasis model

Thirteen five- to six-week-old female BALB/c mice were randomly divided into two groups and implanted with 4T1-luc-Topo cells (n = 6) or 4T1-luc-Cytl1 cells (n = 7) through the injection of 1×10^6 cells in 100 μl of PBS into the fourth mammary fat pads (MFPs) of each mouse. After 30 days, D-luciferin (PerkinElmer, USA) was injected into the abdominal cavity of the mice, and 12 min after the injection, tumor growth and metastasis were monitored *in vivo* through fluorescence intensity measurements using the IVIS Spectrum Imaging System. All the mice were then sacrificed, and the lungs were removed and stained with Bouin's solution for 24 h. The visible disseminated nodules in the lungs were counted. The orthotopic tumors were removed, the tumor sizes were measured, and the tumors were fixed in 10% formalin. The lungs and orthotopic tumors were then subjected to H&E staining and immunohistochemistry (IHC).

IHC

The immunohistochemical analysis was performed using formalin-fixed, paraffin-embedded mouse tissues as previously described.[24] Antibodies against p-STAT3 (Y705) (Cell Signaling Technology, Danvers, MA, USA) were used as primary antibodies.

Statistical analysis

The data are expressed as the mean ± SEMs. The statistical analyses were performed using two-tailed Student's t-tests (unpaired) with Prism 5.0 (GraphPad Software, San Diego, CA, USA). The significant differences between groups are represented by *$P < 0.05$, **$P < 0.01$, and ***$P < 0.001$.

Results

CYTL1 is downregulated in multiple types of tumors

To fully understand the expression pattern of CYTL1 in tumors, we first analyzed the GEO database. The results showed that compared with benign prostatic hyperplasia tissue, CYTL1 was downregulated in primary tumors of human prostate cancer, and this downregulation was more pronounced in metastatic tumors (GDS1439/219837_s_at, Figure 1a). CYTL1 was also downregulated in the N-methyl-N-nitrosourea-induced rat breast cancer model (GDS1363/1375001_at, Figure 1b). A similar result was found for the SP-C/c-raf transgenic mouse model of lung cancer (GDS3826/1456793_at, Figure 1c). To further assess the expression of CYTL1 in tumors, we performed an integrated bioinformatics analysis based on a dataset from the TCGA and GEO databases to determine the differential expression of CYTL1 across multiple cancers and corresponding control tissues (normal or non-tumor) at the mRNA level. The data from the TCGA database (Figure 1d) and the GEO database (Table 1) were consistent and showed that CYTL1 was generally downregulated in most types of tumors. The results obtained from the analysis of the GEO database showed that CYTL1 was significantly downregulated in breast invasive carcinoma, prostate adenocarcinoma, lung squamous cell carcinoma, lung

adenocarcinoma, and stomach adenocarcinoma, among other tumors. The expression of CYTL1 was unchanged in thyroid carcinoma and kidney renal papillary cell carcinoma and upregulated in kidney renal clear cell carcinoma and liver hepatocellular carcinoma. Rank-based box plots of the expression of this gene in these tumors were generated (Figure 1e–i and Supplementary Figure 1a-k). Because it is well known that DNA methylation in promoters silences the corresponding genes, the hypermethylation of *CYTL1* was further analyzed based on the TCGA database, and we found that *CYTL1* was generally hypermethylated at different methylation sites in breast invasive carcinoma, prostate adenocarcinoma, lung squamous cell carcinoma and lung adenocarcinoma (Figure 1j–m), as well as bladder urothelial carcinoma and colon adenocarcinoma (Supplementary Figure 1l-m).

We then analyzed the CYTL1 expression profile in human normal tissues by qPCR and found that CYTL1 was highly expressed in normal placenta, lung, prostate and lymph tissues (Figure 2a). CYTL1 exhibited a high expression level in the lung, and its expression was decreased in lung cancer with high methylation. We subsequently examined the expression of CYTL1 in paired lung cancer tissues and adjacent normal tissues. Specifically, we analyzed CYTL1 expression in randomly selected samples by PCR (4 pairs) and qPCR (8 pairs) and found that CYTL1 expression was markedly downregulated (Figure 2b–c). Furthermore, CYTL1 expression in 60 pairs of tissues was examined by western blotting. Compared with non-tumor tissues, CYTL1 expression was downregulated in 51 pairs of lung cancer tissues (85%). The western blotting results obtained with polyclonal antibody against CYTL1 showed two bands at 19 and 26 kDa, and lung cancer tissues showed lower expression of both bands. The protein expression level of CYTL1 was consistent with the PCR and qPCR results obtained using randomly selected samples. The western blotting results of six representative paired tissues are shown in Figure 2d. In addition, a quantitative analysis of the western blotting results of all 60 paired tissues was performed by normalizing the band density of CYTL1 (26 kDa) to that of β-actin. The relative CYTL1 expression levels in tumor versus paired adjacent non-tumor tissues were calculated (Figure 2e).

Overexpression of CYTL1 inhibits the migration and invasion of A549 cells

The downregulation of CYTL1 in lung cancer tissues and mouse model suggested that it might play tumor-suppressive roles. To study the function of CYTL1 in lung cancer, we overexpressed CYTL1 in A549 cells and detected its effects on cell proliferation and migration.

First, we transiently overexpressed CYTL1 in A549 cells using the expression vector pcDNA3.1-CYTL1-his and performed CCK-8, Transwell and wound-healing assays. The results showed that the overexpression of CYTL1 could only slightly inhibit the proliferation of A549 cells but led to a marked decrease in migration (Supplementary Figure 2).

Subsequently, stable CYTL1-expressing A549 cells were generated (Figure 3a) using the lentiviral vectors TG006-Native-CYTL1 (CYTL1 with its native signal peptide) and
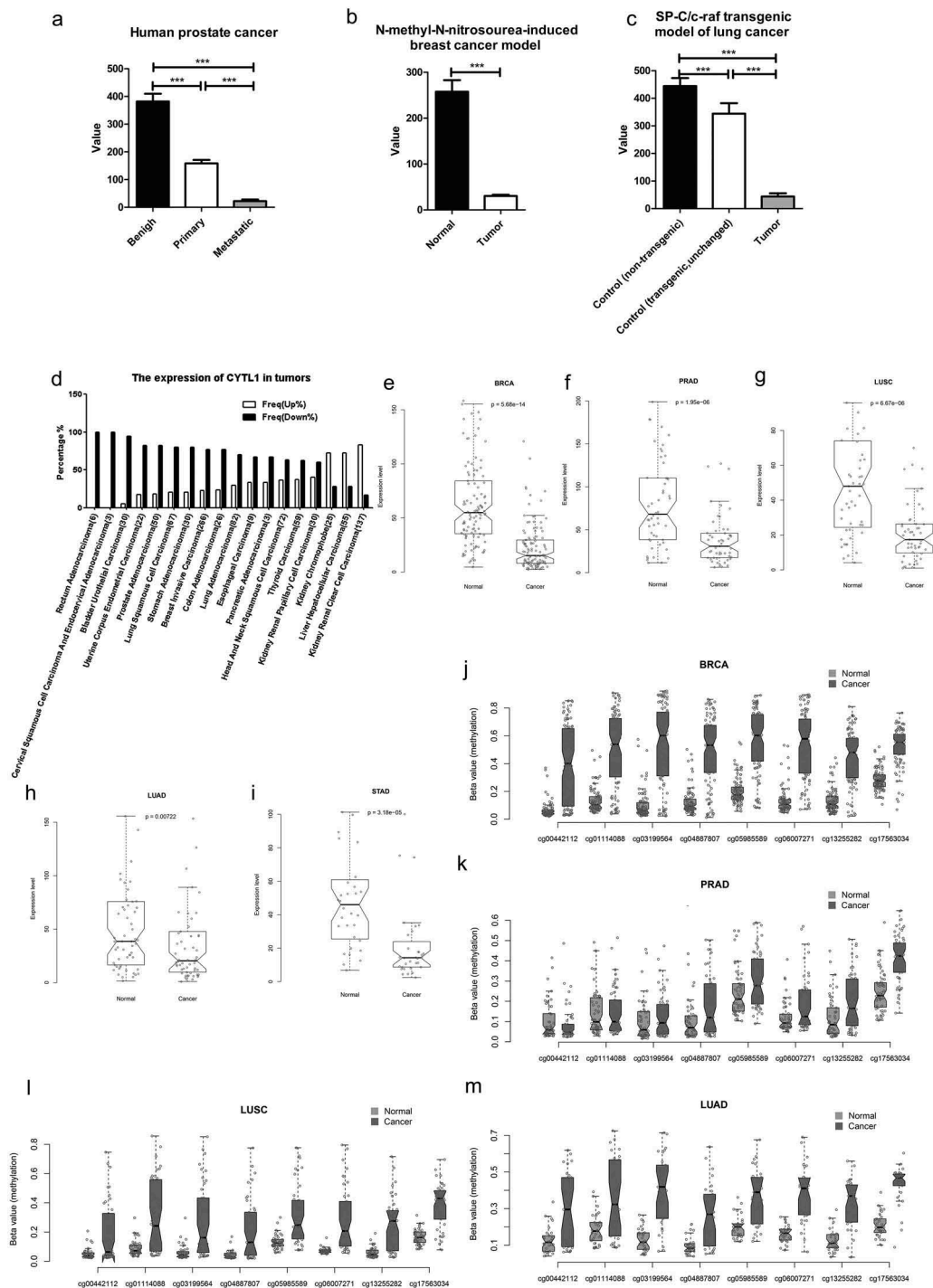
Figure 1. CYTL1 is downregulated in multiple types of tumors.

(a–c). Expression of CYTL1 in human prostate cancer (GDS1439/219837_s_at, a), the N-methyl-N-nitrosourea-induced rat breast cancer model (GDS1363/1375001_at, b) and the SP-C/c-raf transgenic mouse model of lung cancer (GDS3826/1456793_at, c) based on an analysis of the GEO database. The value in the y axis represents the expression level of CYTL1. The value within a GEO DataSet have been calculated in an equivalent manner and normalized using a wide variety of methods according to the original submitter-supplied sample records. (d). Expression of CYTL1 in various tumors based on an analysis of the TCGA database. % represents the proportion of tumor cases with upregulation or downregulation of CYTL1. (e–i). Expression of CYTL1 in breast invasive carcinoma (e), prostate adenocarcinoma (f), lung squamous cell carcinoma (g), lung adenocarcinoma (h) and stomach adenocarcinoma (i) based on an analysis of the GEO database. (j–m). Hypermethylation of *CYTL* in breast invasive carcinoma (j), prostate adenocarcinoma (k), lung squamous cell carcinoma (l) and lung adenocarcinoma (m) based on an analysis of the TCGA database. The beta value in the y axis is the ratio of the methylated probe intensity and the overall intensity (sum of methylated and unmethylated probe intensities) and represents the methylation levels.

TG006-Igκ-CYTL1 (CYTL1 with the Igκ signal peptide). We verified that replacement of the signal peptide with the mouse Igκ signal peptide increased the expression level of CYTL1.[7] As shown in Figure 3a, the expression of CYTL1 was increased in both the lysate and the supernatant of A549-Igκ-CYTL1 cells compared with those of the A549-Native-CYTL1 cells. Using these two types of cells and A549 cells infected with the TG006 lentivirus as a control group, proliferation

Table 1. The expression of CYTL1 in tumors analyzed in the GEO database.

	Tumor type	p value (cancer vs normal or non tumor)
Downregulated	BRCA (Breast invasive carcinoma)	5.68E-14
	PRAD (Prostate adenocarcinoma)	1.95E-06
	LUSC (Lung squamous cell carcinoma)	6.67E-06
	STAD (Stomach adenocarcinoma)	3.18E-05
	BLCA (Bladder Urothelial Carcinoma)	7.25E-05
	COAD (Colon adenocarcinoma)	0.005133182
	HNSC (Head and Neck squamous cell carcinoma)	0.006333946
	LUAD (Lung adenocarcinoma)	0.007218447
	READ (Rectum adenocarcinoma)	0.03125
Unchanged	UCEC (Uterine corpus endometrial carcinoma)	0.296875
	THCA (Thyroid carcinoma)	0.328340042
	ESCA (Esophageal carcinoma)	0.764648438
	KIRP (Kidney renal papillary cell carcinoma)	0.933870792
Upregulated	KIRC (Kidney renal clear cell carcinoma)	4.29E-09
	LIHC (Liver hepatocellular carcinoma)	0.00026157
	KICH (Kidney chromophobe)	0.042150199

assessed by CCK-8 kit, migration and invasion, assessed either using transwell or wound-healing assays, were conducted. The absorbance of the CCK-8 reagent, which is proportional to the number of cells, increased with time similarly in A549-Native-

CYTL1, A549-Igk-CYTL1 and control cells (Figure 3b), suggesting that CYTL1 barely inhibited the proliferation of A549 cells. The decreased migrated cells of CYTL1-overexpression groups in Transwell assays and retarded wound closures of CYTL1-overexpression groups in wound-healing assays suggested that CYTL1 significantly inhibited the migration of A549 cells (Figure 3c–d). The decreased migrated cells of CYTL1-overexpression groups in invasion assays suggested the invasion inhibitory effects of CYTL1 in A549 cells (Figure 3e). Notably, CYTL1 more strongly inhibited the migration and invasion of A549-Igκ-CYTL1 cells, indicating that CYTL1 exerts dose-dependent effects.

Recombinant CYTL1 inhibits migration and STAT3 phosphorylation in various tumor cells

CYTL1 is a secreted protein that is downregulated in lung, breast and prostate cancer, as consistently demonstrated through analyses of the GEO and TCGA databases, and this finding was experimentally verified in lung cancer tissues. We demonstrated that the overexpression of CYTL1 could inhibit A549 cell migration. To further determine the function of CYTL1, A549 cells were treated with recombinant CYTL1 protein, which was expressed and purified from CHO cells,[7] and the CCK-8, Transwell, wound-healing and invasion assays were then conducted to access the proliferation, migration and invasion of A549 cells respectively. The similar
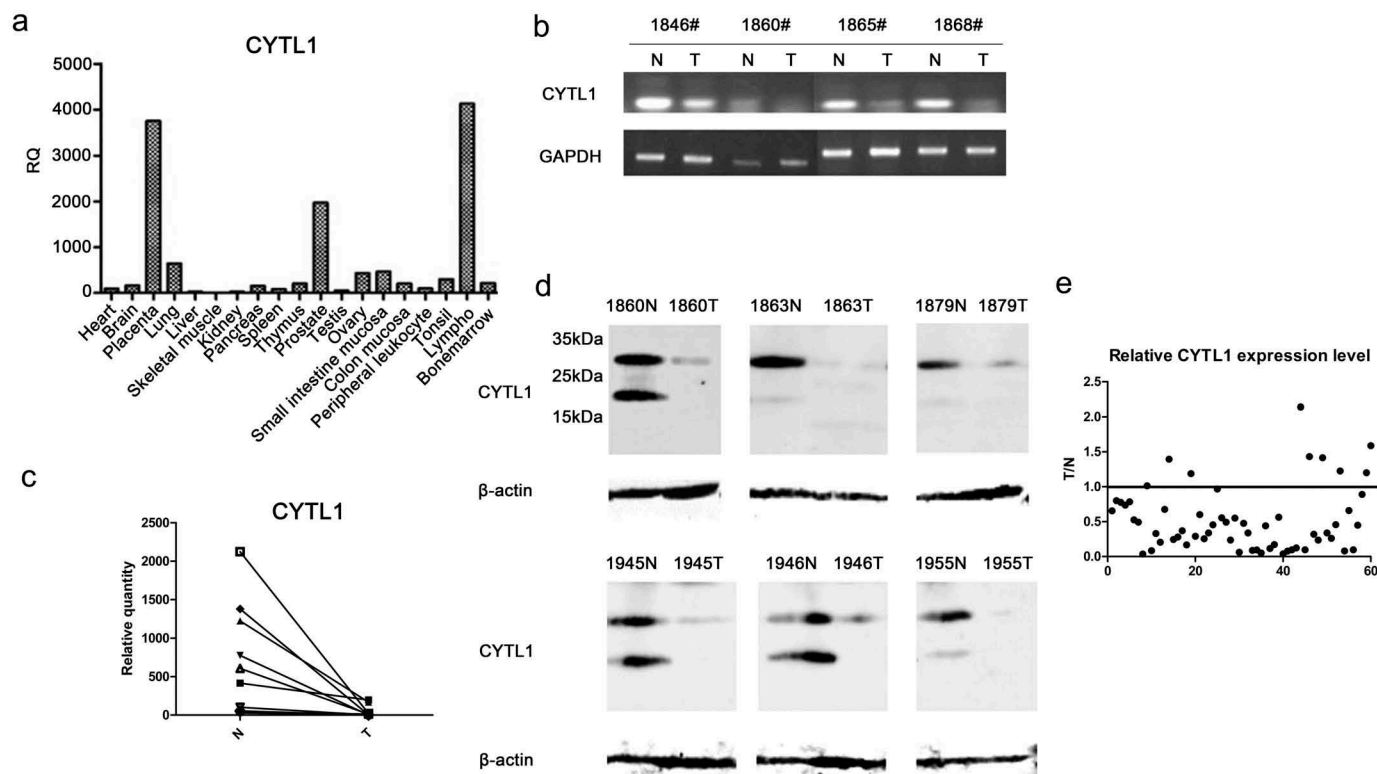

Figure 2. CYTL1 is frequently downregulated in lung cancer tissues. (a). The CYTL1 expression profile in human normal tissues was detected by qPCR. (b, c). The expression of CYTL1 in tumor (T) and paired adjacent non-tumor (N) tissues was detected by PCR (b), and that in representative samples was detected by qPCR (c). In the qPCR analysis, the CYTL1 expression level in the 1860# tumor tissue was set to 1, and GAPDH was used as an internal control. (d). CYTL1 expression was further examined by western blotting. The results for six representative paired tissues are shown. β-actin was used as an internal standard. (e). The relative CYTL1 expression level in all 60 patients was calculated as the tumor versus paired adjacent non-tumor tissue (T/N) values according to the western blotting results. A dot is used to represent the value for each sample.
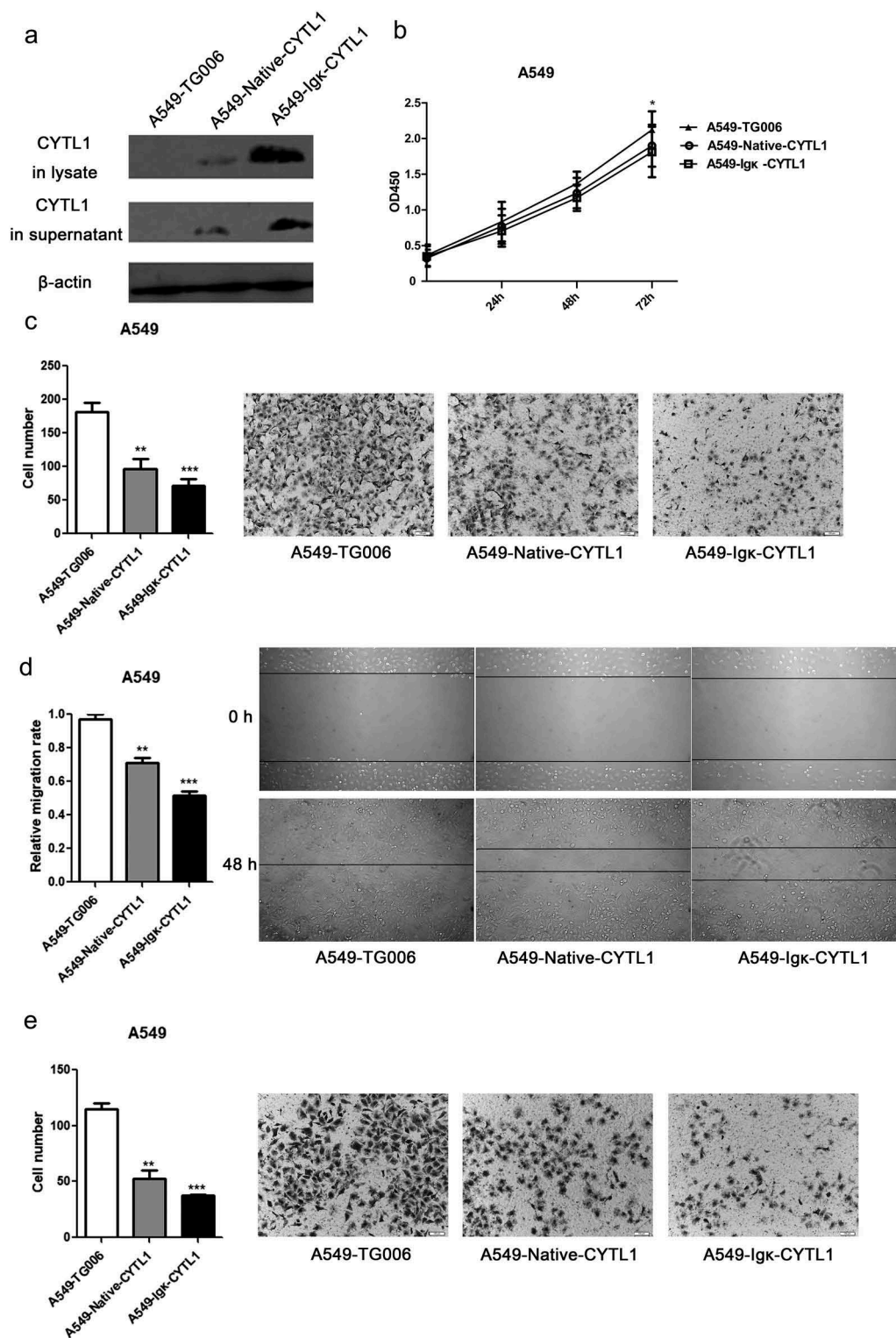
Figure 3. Overexpression of CYTL1 inhibits lung cancer cell (A549) migration and invasion. (a). The overexpression of CYTL1 by the lentiviral vectors TG006-Native-CYTL1 and TG006-Igκ-CYTL1 was confirmed by western blotting. The empty vector (TG006) was used as a control. (b–e). CCK-8 (b), Transwell (c), wound-healing (d) and invasion assays (e) were performed. Representative images of A549 cell migration obtained from the Transwell, invasion (magnification × 200) and wound-healing (magnification × 100) assays are shown (*right*). The cell numbers obtained from the Transwell and invasion assays were counted, and the relative migration rate obtained from the wound-healing assays was calculated by dividing the change in the distance between the scratch edges by the initial distance (*left*). The results are expressed as the means±SEMs from three independent experiments conducted in triplicate. * $P < 0.05$, ** $P < 0.01$, and *** $P < 0.001$ compared with the controls at each time point.

absorbance curves of the CCK-8 assay showed that recombinant CYTL1 exerted no obvious effect on proliferation (Figure 4a). However, compared with the control group, the cell numbers in recombinant CYTL1-treated groups significantly decreased in the transwell membranes treated with (Figure 4b) or without (Figure 4d) matrigel, suggesting that CYTL1
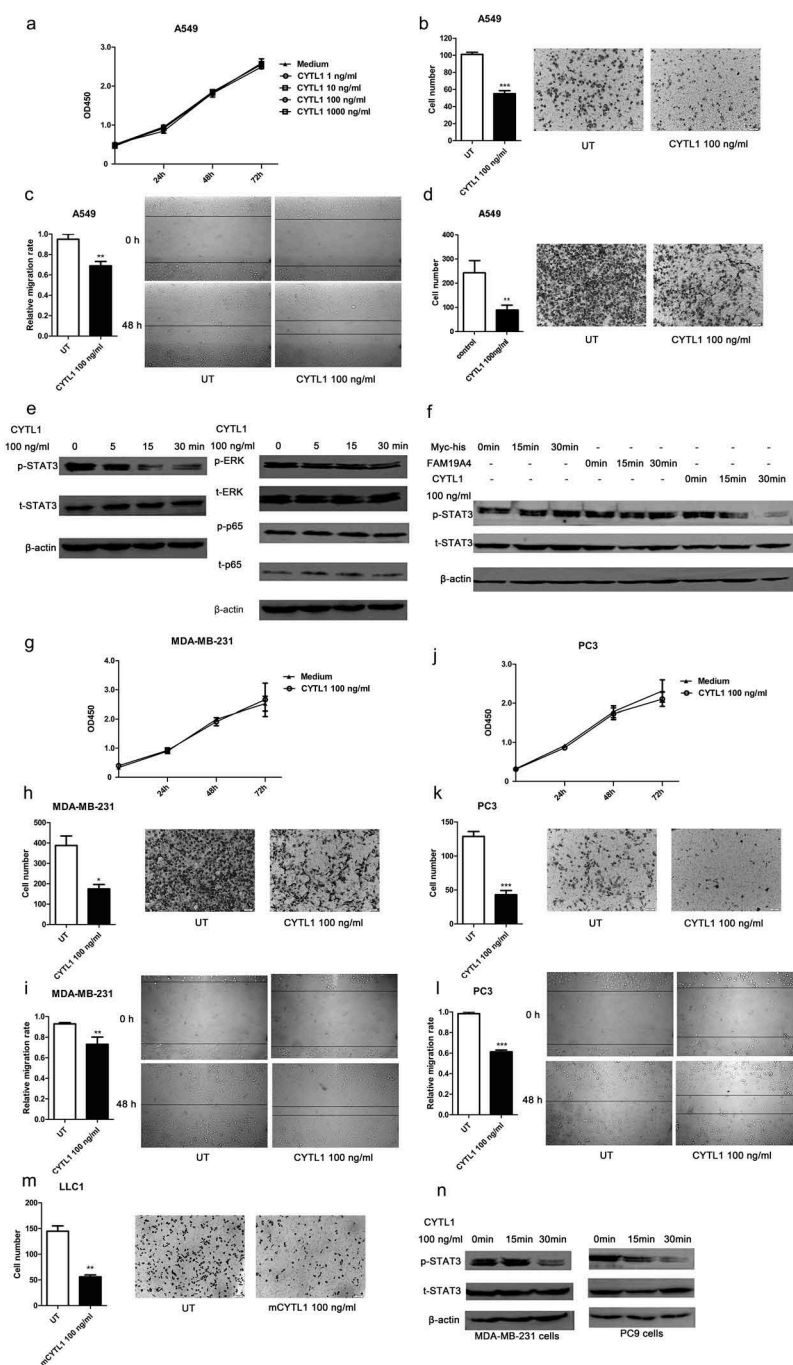
Figure 4. Recombinant CYTL1 protein inhibits migration and STAT3 phosphorylation in various tumor cells. (a–d). A549 cells were treated with CYTL1 protein, and the culture medium was used as a control. CCK-8 (1, 10, 100, and 1000 ng/ml CYTL1) (a), Transwell (b), wound-healing (c) and invasion (100 ng/ml CYTL1) (d) assays were performed. e. Phosphorylation of STAT3, ERK and p65 in A549 cells treated with 100 ng/ml CYTL1 for 5, 15, or 30 min. (f). Specific effect of CYTL1 on STAT3 phosphorylation in A549 cells. FAM19A4 and Myc-his were used as controls. (g–i). CCK-8 (g), Transwell (h) and wound-healing (i) assays of MDA-MB-231 cells (100 ng/ml CYTL1) were performed. (j–l). CCK-8 (j), Transwell (k) and wound-healing (l) assays of PC3 cells (100 ng/ml CYTL1) were performed. m. Transwell assays of LLC1 cells (100 ng/ml mouse CYTL1) were performed. Representative images of tumor cell migration obtained from the Transwell, invasion (magnification × 200) and wound-healing (magnification × 100) assays are shown (*right*). The cell numbers obtained from the Transwell and invasion assays were counted, and the relative migration rate obtained from the wound-healing assays was calculated by dividing the change in the distance between the scratch edges by the initial distance (*left*). The results are expressed as the means±SEMs from three independent experiments conducted in triplicate. * $P < 0.05$, ** $P < 0.01$, and *** $P < 0.001$ compared with the controls at each time point. (n). Effect of CYTL1 (100 ng/ml) on STAT3 phosphorylation in MDA-MB-231 and PC9 cells.

significantly inhibited the migration (Figure 4b) and invasion (Figure 4d) of this cell line. Moreover, the wound-healing assays revealed that wound closure was retarded in the CYTL1-treated A549 cells (Figure 4c). These results indicate that recombinant CYTL1 could inhibit the migration and invasion of A549 cells.

Subsequently, we explored the mechanism underlying the inhibitory effect of CYTL1 on migration. We treated A549 cells with 100 ng/ml CYTL1 and detected the activation of various signal pathways. The western blotting results suggested that CYTL1 exerted a strong inhibitory effect on the phosphorylation of STAT3 within 15 and 30 min but

had no effect on ERK and p65 (Figure 4e). To further verify the effect of CYTL1, we treated A549 cells with the control protein FAM19A4 (another novel cytokine identified in our immunogenomics-based screening platform)[25] or the Myc-his peptide and found that these treatments had no effect on STAT3 phosphorylation (Figure 4f). STAT3 is an important transcription factor and signaling molecule involved in tumor development and metastasis.[19] CYTL1 might exert its inhibitory effect on migration by inhibiting the phosphorylation of STAT3.

Our results demonstrated that CYTL1 inhibited the migration and invasion of A549 cells and that CYTL1 was significantly downregulated in various types of tumors, such as breast and prostate cancer. Therefore, to further explore the inhibitory effect of CYTL1 in tumors and to study its effect on other cancer cells, we subsequently detected the effect of CYTL1 on the proliferation and migration of other cancer cells by treating various cells with recombinant CYTL1 and performing CCK-8, Transwell and wound-healing assays. The results showed that CYTL1 exerted a similar inhibitory effect on the migration of MDA-MB-231 cells (breast cancer cell line; Figure 4g–i), PC3 cells (prostate cancer cell line; Figure 4j–l) and LLC1 cells (mouse Lewis lung carcinoma cell line; Figure 4m). Hence, the results verify that CYTL1 inhibits the migration of multiple cancer cell lines.

Due to the inhibitory function of CYTL1 in multiple tumor cells, we also detected the phosphorylation of STAT3 in MDA-MB-231 and PC9 cells treated with CYTL1 protein. As shown in Figure 4n, CYTL1 could inhibit STAT3 phosphorylation in these tumor cell lines.

We have verified that CYTL1 inhibited the migration of multiple types of tumor cells. Both CYTL1 overexpression in tumor cells and treatment with CYTL1 protein revealed that CYTL1 exerted a similar inhibitory effect on migration. Therefore, CYTL1 might exert its function through a specific receptor in tumor cells. In a previous study, we confirmed that CYTL1 exhibited chemotactic activity on monocytes/macrophages through CCR2.[9] To determine whether CYTL1 exerts its tumor-suppressing effect through CCR2 in tumor cells, we first detected CCR2 expression in A549 cells. Results in Figure 5a–b showed a low level of CCR2 in A549 cells. Transwell assays of A549 cells treated with CYTL1 only or combined with the CCR2 antagonist RS504393 were performed. The results showed that the CCR2 antagonist did not reverse the inhibitory effect of CYTL1 (Figure 5c), indicating that CYTL1 inhibited the metastasis of tumor cells through other receptors, which remains to be identified. In addition, Jooyeon Kim et al demonstrated that the promotion effect of CYTL1 on cardiac fibrosis was completely abrogated by co-treatment with SB-431542, an antagonist of TGF-β receptor 1.[26] These results suggested that TGF-β receptor 1 might be a functional receptor of CYTL1. However, our western blotting results showed that SB-431542 did not reverse the inhibitory effect of CYTL1 on STAT3 (Figure 5d).

CYTL1 suppresses breast cancer metastasis *in vivo*

The bioinformatics analysis showed that CYTL1 was significantly downregulated in multiple types of tumors, including breast cancer. The inhibitory activities of CYTL1 in the migration of MDA-MB-231 cells were also demonstrated experimentally *in vitro*. Subsequently, we used mouse breast cancer models to confirm the *in vivo* tumor-suppressing activity of CYTL1. We constructed 4T1-luc cells stably expressing mouse Cytl1 (4T1-luc-Cytl1) (Supplementary Figure 3A) and examined the effect of Cytl1 on proliferation and migration *in vitro*. The results of the CCK-8, Transwell and wound-healing assays showed that Cytl1 inhibited the migration of the constructed 4T1-luc cells but had no effect on their proliferation (Supplementary Figure 3B-D).

Subsequently, we constructed a mouse breast cancer experimental metastasis model by injecting 4T1-luc-Cytl1 cells and control 4T1-luc-Topo cells into BALB/c mice via the tail veins. Nine days after injection, the tumors were monitored using the IVIS Spectrum Imaging System, and results showed that tumor growth and metastasis were inhibited in the 4T1-luc-Cytl1 group (Figure 6a). Figure 6b shows the fluorescence intensity of the two groups. The lungs were subjected to Bouin's and H&E staining, and as shown in Figure 6c–d, the tumor nodules and areas in the control group were greater than those in the Cytl1-overexpressing group. Figure 6e shows the statistical results of the analysis of the tumor area in the lungs. We also monitored the survival of the mice in the two groups and found that Cytl1-overexpression in the experimental metastasis model could increase the survival rate of mice (Figure 6f).

We also constructed a spontaneous metastasis model of breast cancer by injecting the same cells into the MFPs of BALB/c mice. Thirty days later, we observed tumor growth and metastasis using the IVIS Spectrum Imaging System and found no significant difference in the orthotopic tumors (Figure 7a–c), but the tumor metastasis in the 4T1-luc-Cytl1 group was notably decreased. Figure 7b shows the fluorescence intensity of the metastatic tumors in the two groups. The lungs of the mice in the two groups were subjected to Bouin's and H&E staining, and as shown in Figure 7d and f, the tumor nodules and areas in the Cytl1-overexpressing group were markedly increased compared with those in the control group. Figure 7e–g show the statistical results of the tumor nodule numbers and areas in the lungs, respectively.

To further explore the tumor-suppressing function and mechanism of CYTL1 in the mouse breast cancer models, we detected the expression of p-STAT3 and CD68 in orthotopic tumors and lung tissues from spontaneous metastasis model mice by IHC. Cytl1 decreased the phosphorylation of STAT3 in both the orthotopic tumors and lung tissues, which was consistent with the *in vitro* function of CYTL1 (Figure 7h). We analyzed the infiltration of tumor associated macrophages (TAMs) by detecting CD68 expression, but there was no significant difference (Figure 7i).
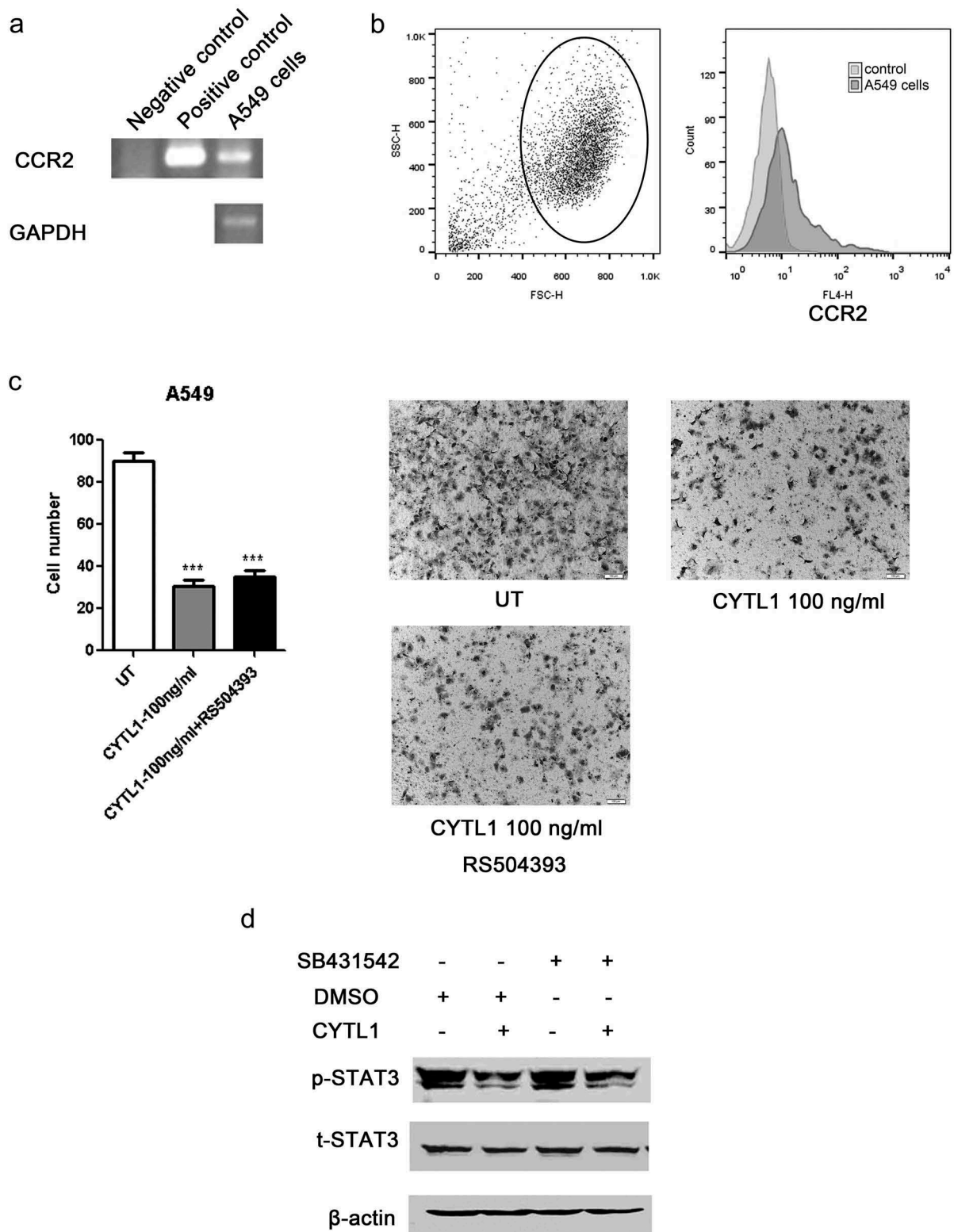
Figure 5. CCR2 antagonist does not reverse the inhibitory effect of CYTL1 on migration. (a, b). CCR2 expression in A549 cells was detected by PCR (a) and FACS (b). (c). Transwell assays of A549 cells treated with RS504393 were performed. Representative images of A549 cell migration obtained from the Transwell assay (magnification × 200) are shown (*right*), and the cell numbers obtained from the Transwell assays were counted (*left*). The results are expressed as the means±SEMs from three independent experiments conducted in triplicate. * $P < 0.05$, ** $P < 0.01$, and *** $P < 0.001$ compared with the controls. (d). Effect of CYTL1 (100 ng/ml) on STAT3 phosphorylation in A549 cells treated with SB-431542.

We have demonstrated that CYTL1 could directly inhibit the migration of tumor cells and the significant decrease of tumor metastasis in CYTL1 group *in vivo* studies was consistent with the *in vitro* CYTL1 function. Therefore, we suppose that CYTL1 acts by inhibiting the metastasis of breast cancer *in vivo* according to the above-mentioned data.
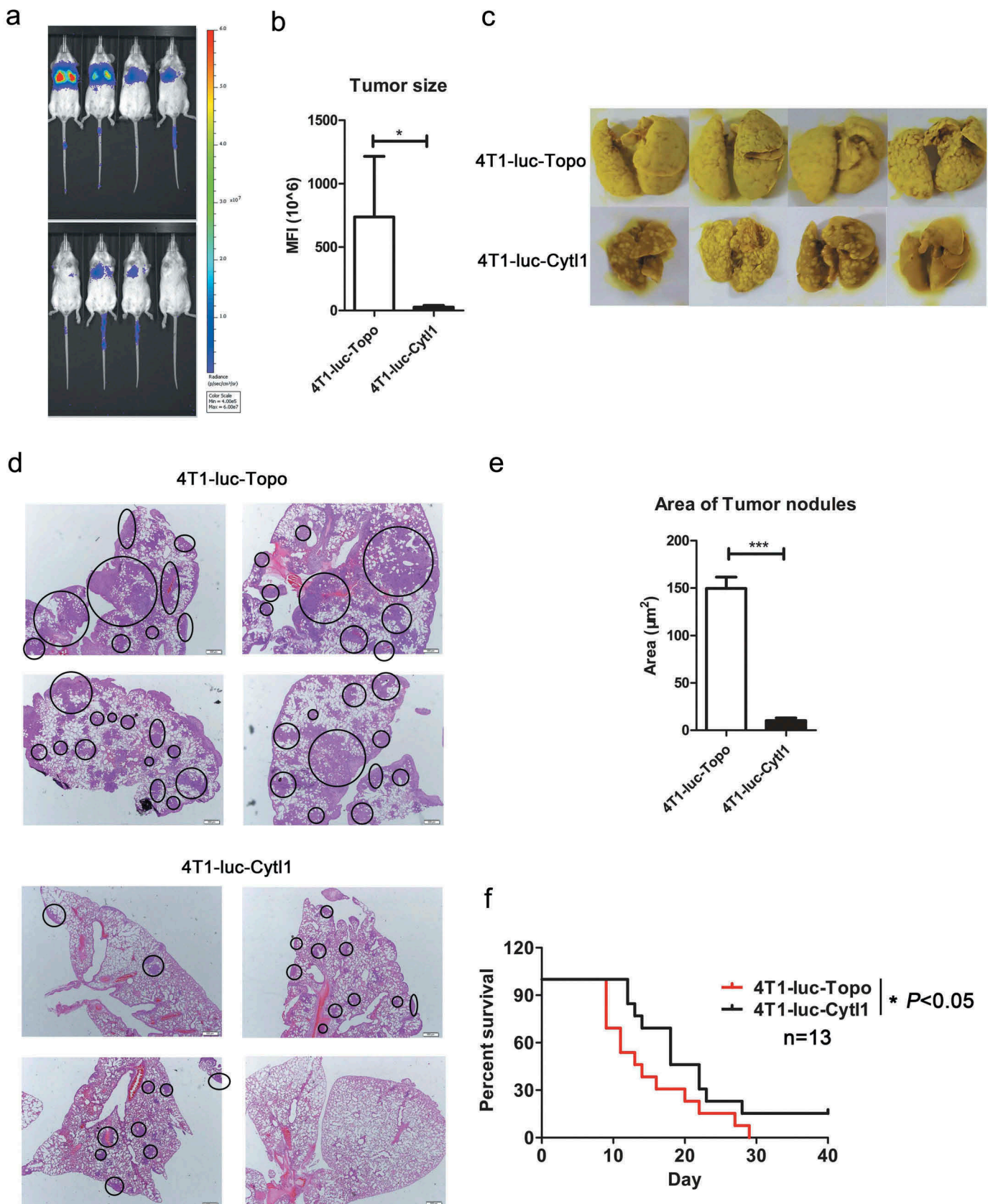
Figure 6. CYTL1 suppresses tumor metastasis and increases the survival rate in a mouse experimental metastasis model of breast cancer. (a). Tumor metastasis in the lung was monitored using the IVIS Spectrum Imaging System. (b). The fluorescence intensity was quantified and is shown in bar graphs (n = 4). (c). The tumor nodules in the lungs were observed by Bouin's staining. d. The tumor nodules in the lungs were observed by H&E staining. (e). The area of the metastasizing tumors was calculated according to the H&E staining results. (f). Survival curve of tumor-bearing mice (n = 13). * P < 0.05, ** P < 0.01, and *** P < 0.001 compared with the controls at each time point.
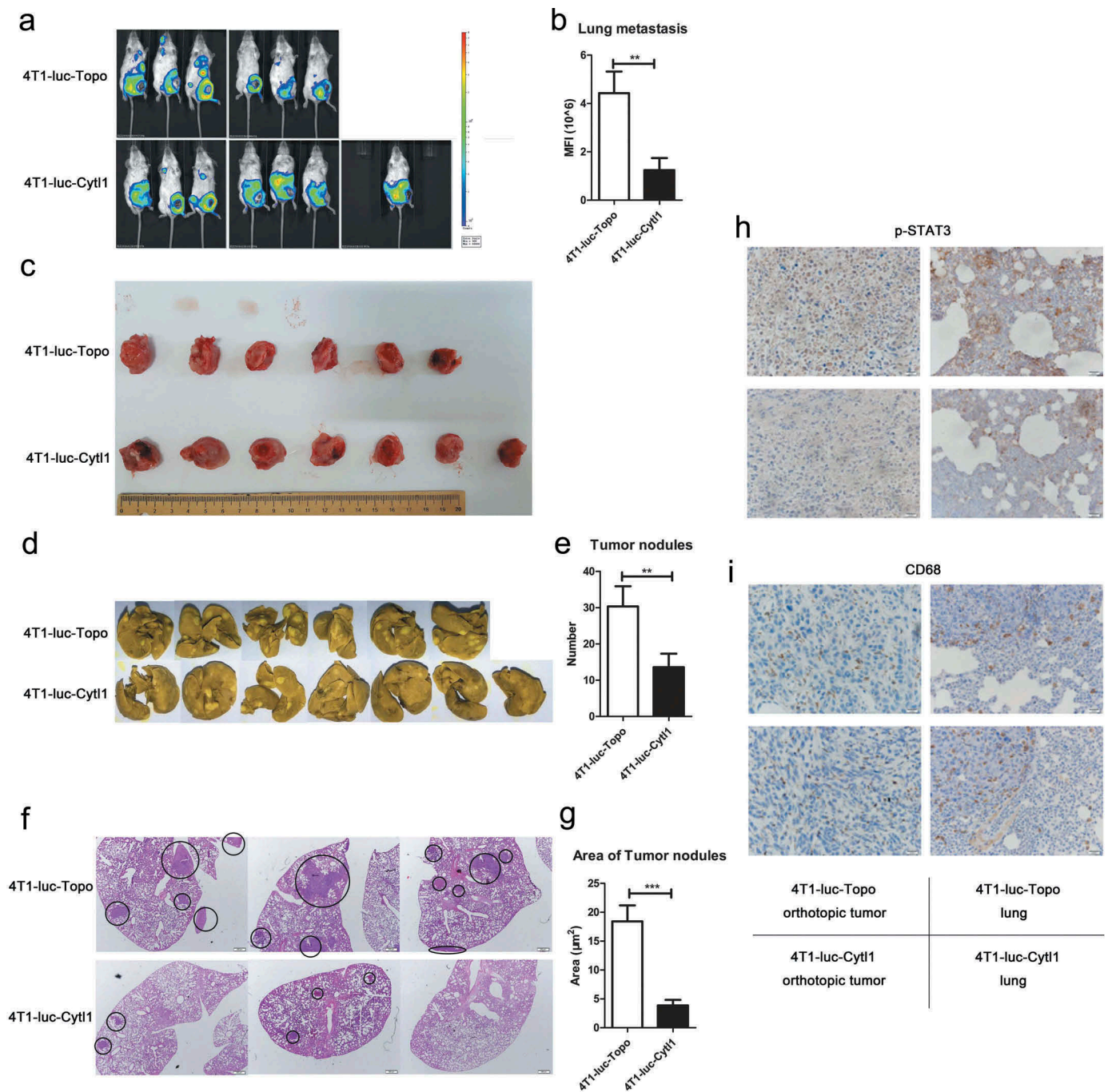
Figure 7. CYTL1 suppresses tumor metastasis and STAT3 phosphorylation in a mouse spontaneous metastasis model of breast cancer. (a). Tumor growth and metastasis were monitored using the IVIS Spectrum Imaging System. (b). Metastasis was quantified through an analysis of fluorescence intensity and shown by bar graphs (4T1-luc-Topo cells (n = 6), 4T1-luc-Cytl1 cells (n = 7)). (c). The orthotopic tumors were dissected and photographed. (d). The tumor nodules in the lungs were observed by Bouin's staining. (e). Disseminated nodules larger than or equal to 1 mm in diameter were counted, and the data are shown by bar graphs. (f). The tumor nodules in the lungs were observed by H&E staining. g. The area of the metastasizing tumors was calculated according to the H&E staining results. (h, i). The expression of p-STAT3 (h) and CD68 (i) in orthotopic tumors and lung tissues was detected by IHC. * $P < 0.05$, ** $P < 0.01$, and *** $P < 0.001$ compared with the controls at each time point.

Discussion

CYTL1 is a novel cytokine that performs multiple functions. To elucidate the expression and function of CYTL1 in tumors, we performed a comprehensive analysis of CYTL1 across multiple cancers using bioinformatics approaches. The results indicated that CYTL1 was significantly downregulated in breast, prostate, lung and stomach cancer, which was consistent with the hypermethylation of

CYTL1 in these tumors. Decreased mRNA and protein expression of CYTL1 was observed in lung cancer tissues. Our data suggested that CYTL1 played an inhibitory role in lung, prostate and breast cancer cell migration and that this effect was accompanied by a reduction of STAT3 phosphorylation. The *in vivo* research also verified that CYTL1 inhibited breast cancer metastasis. In this study, we confirmed that CYTL1 is a tumor-suppressing cytokine. The

function of CYTL1 in tumors with unchanged or upregulated CYTL1 expression remains to be further studied.

The western blotting of lung cancer and normal tissues detected two CYTL1 bands, i.e., 19 kDa and 26 kDa, and decreased expression of both bands was observed in lung cancer tissues, which might be due to post-translational modification of the CYTL1 protein. The study performed by Xuan Liu detected two CYTL1 bands in lysates (19 kDa and 40 kDa) of HEK293T cells overexpressing CYTL1 but only one specific band in the supernatant (26 kDa),[1] suggesting a modification of secreted CYTL1. However, based on the amino acid sequence, CYTL1 contains no potential N-glycosylation sites. Digestion with a panel of glycosidases showed no effect on the molecular size of CYTL1.[1] The nature of the putative modification remains to be determined.

In a previous study, we confirmed that CYTL1 exhibited chemotactic activity on monocytes/macrophages through CCR2.[9] The CCL2/CCR2 axis plays an important role in tumorigenesis and tumor metastasis in many types of tumors, including lung cancer,[27] breast cancer[28] and prostate cancer.[29] However, our results showed that CYTL1 inhibited the metastasis of tumor cells through other receptors instead of CCR2. We also found that CYTL1 had no effect on recruiting TAM infiltration. In our opinions, CYTL1 is inclined to act by inhibiting tumor cell metastasis in breast cancer models. On the other hand, TGF-β receptor 1 antagonist SB-431542 did not reverse the inhibitory effect of CYTL1 on STAT3. Further research is required to explore the functional receptors of CYTL1 in tumor cells.

It was recently proven that IL-24 inhibits lung cancer cell migration and invasion by disrupting the SDF-1/CXCR4 signaling axis.[14] IL-37 has also been demonstrated to mediate antitumor activity through the suppression of IL-6/STAT3 signaling in human cervical cancer cells and renal carcinoma cells.[30] Cytokines belonging to the IL-6 family and ligands of receptor tyrosine kinases, such as epidermal growth factor and vascular endothelial growth factor, are the main activators of STAT3 in tumors.[31] These factors activate the STAT3 signaling pathway by binding to specific receptors and activating downstream signals. For example, IL-6 mediates the phosphorylation of a tyrosine residue (Y705) of STAT3 and regulates the proliferation, migration, apoptosis, immune response, angiogenesis and metastasis of cancer cells by modulating the expression of downstream target genes. IL-6 exerts its function by binding IL-6Rα (IL-6 receptor-α) and activates downstream signals through gp130 (glycoprotein 130 or IL-6Rβ).[32,33] CYTL1 likely impacts the binding of ligands and receptors or downstream signal transduction, thus inhibiting STAT3. However, STAT3 also has some negative regulation mechanisms. For example, protein-tyrosine-phosphatase (PTP),[34] the suppressors of cytokine signaling (SOCS) family[35] and the protein inhibitors of activated STAT (PIAS) family[36] can inhibit STAT3 phosphorylation, and Oncostatin M was recently proven to suppress tumor metastasis in lung adenocarcinoma by suppressing the activating effect of STAT3-dependent signaling via PIAS3.[37] It is also possible that CYTL1 inhibits STAT3 by enhancing the negative regulation of STAT3. The mechanism through which CYTL1 inhibits STAT3 phosphorylation requires further research.

Many cytokines, such as IL-24 and IL-37, exert tumor-suppressing effects and related clinical trials of tumor treatment have been conducted.[15,18] In our article, we demonstrated that both recombinant CYTL1 and overexpression of CYTL1 could inhibit the migration of multiple types of tumor cells. It is possible that the tumor-suppressing cytokine CYTL1 might be used in tumor treatment, such as lung cancer and breast cancer. In addition, bioinformatics analyses showed that CYTL1 was downregulated in multiple types of tumors and our results showed a remarkable decrease of CYTL1 in lung caner at mRNA and protein levels. The expression of CYTL1 might serve as a marker for tumor diagnosis. First of all, it is necessary to detect the concentration of CYTL1 in serum of tumor patients. However, CYTL1 is a novel cytokine. The detection method of CYTL1 in serum or supernatant has not been established, which needs further researches. The analysis of CYTL1 concentration in patient serum will contribute to the applications for tumor diagnosis and treatment.

Conclusions

To summarize, CYTL1 inhibits the migration of multiple types of tumors with decreasing phosphorylation of STAT3. CYTL1 is a tumor-suppressing cytokine.

Disclosure of Potential Conflicts of Interest

No potential conflicts of interest were disclosed.

Funding

References

1. Liu X, Rapp N, Deans R, Cheng L. Molecular cloning and chromosomal mapping of a candidate cytokine gene selectively expressed in human CD34+ cells. Genomics. 2000;65 (3):283–292. PMID: 10857752. doi:10.1006/geno.2000.6170.
2. Hermansson M, Sawaji Y, Bolton M, Alexander S, Wallace A, Begum S, Wait R, Saklatvala J. Proteomic analysis of articular cartilage shows increased type II collagen synthesis in osteoarthritis and expression of inhibin betaA (activin A), a regulatory molecule for chondrocytes. J Biol Chem. 2004;279 (42):43514–43521. PMID: 15292256. doi:10.1074/jbc. M407041200.
3. Ficker M, Powles N, Warr N, Pirvola U, Maconochie M. Analysis of genes from inner ear developmental-stage cDNA subtraction reveals molecular regionalization of the otic capsule. Dev Biol. 2004;268(1):7–23. PMID: 15031101. doi:10.1016/j. ydbio.2003.11.023.
4. Kim JS, Ryoo ZY, Chun JS. Cytokine-like 1 (Cytl1) regulates the chondrogenesis of mesenchymal cells. J Biol Chem. 2007;282 (40):29359–29367. PMID: 17644814. doi:10.1074/jbc. M700965200.
5. Jeon J, Oh H, Lee G, Ryu JH, Rhee J, Kim JH, Chung KH, Song WK, Chun CH, Chun JS. Cytokine-like 1 knock-out mice (Cytl1-/-) show normal cartilage and bone development but exhibit augmented osteoarthritic cartilage destruction. J Biol Chem.

2011;286(31):27206–27213. PMID: 21652695. doi:10.1074/jbc.M111.218065.

6. Chao C, Joyce-Shaikh B, Grein J, Moshrefi M, Raoufi F, Laface DM, McClanahan TK, Bourne PA, Pierce RH, Gorman DM, et al. C17 prevents inflammatory arthritis and associated joint destruction in mice. PLoS One. 2011;6(7):e22256. PMID: 21799806. doi:10.1371/journal.pone.0022256.

7. Wang X, Liu H, Yuan W, Cheng Y, Han W. Efficient production of CYTL1 protein using mouse IgGkappa signal peptide in the CHO cell expression system. Acta Biochim Biophys Sin (Shanghai). 2016;48(4):391–394. PMID: 26922322. doi:10.1093/abbs/gmw007.

8. Tomczak A, Pisabarro MT. Identification of CCR2-binding features in Cytl1 by a CCL2-like chemokine model. Proteins. 2011;79(4):1277–1292. PMID: 21322034. doi:10.1002/prot.22963.

9. Wang X, Li T, Wang W, Yuan W, Liu H, Cheng Y, Wang P, Zhang Y, Han W. Cytokine-like 1 chemoattracts monocytes/macrophages via CCR2. J Immunol. 2016;196(10):4090–4099. PMID: 27084102. doi:10.4049/jimmunol.1501908.

10. Wen M, Wang H, Zhang X, Long J, Lv Z, Kong Q, An Y. Cytokine-like 1 is involved in the growth and metastasis of neuroblastoma cells. Int J Oncol. 2012;41(4):1419–1424. PMID: 22797702. doi:10.3892/ijo.2012.1552.

11. Kwon YJ, Lee SJ, Koh JS, Kim SH, Lee HW, Kang MC, Bae JB, Kim YJ, Park JH. Genome-wide analysis of DNA methylation and the gene expression change in lung cancer. J Thorac Oncol. 2012;7(1):20–33. PMID: 22011669. doi:10.1097/JTO.0b013e3182307f62.

12. Landskron G, De la Fuente M, Thuwajit P, Thuwajit C, Hermoso MA. Chronic inflammation and cytokines in the tumor microenvironment. J Immunol Res. 2014;2014:149185. PMID: 24901008. doi:10.1155/2014/149185.

13. Menezes ME, Bhatia S, Bhoopathi P, Das SK, Emdad L, Dasgupta S, Dent P, Wang XY, Sarkar D, Fisher PB. MDA-7/IL-24: multifunctional cancer killing cytokine. Adv Exp Med Biol. 2014;818:127–153. PMID: 26811110. doi:10.1007/978-1-4471-6458-6_6.

14. Panneerselvam J, Jin J, Shanker M, Lauderdale J, Bates J, Wang Q, Zhao YD, Archibald SJ, Hubin TJ, Ramesh R. IL-24 inhibits lung cancer cell migration and invasion by disrupting the SDF-1/CXCR4 signaling axis. PLoS One. 2015;10(3):e0122439. PMID: 25775124. doi:10.1371/journal.pone.0122439.

15. Menezes ME, Bhoopathi P, Pradhan AK, Emdad L, Das SK, Guo C, Wang XY, Sarkar D, Fisher PB. Role of MDA-7/IL-24 a multifunction protein in human diseases. Adv Cancer Res. 2018;138:143–182. PMID: 29551126. doi:10.1016/bs.acr.2018.02.005.

16. Xu S, Oshima T, Imada T, Masuda M, Debnath B, Grande F, Garofalo A, Neamati N. Stabilization of MDA-7/IL-24 for colon cancer therapy. Cancer Lett. 2013;335(2):421–430. PMID: 23481022. doi:10.1016/j.canlet.2013.02.055.

17. Liang Z, Yang CS, Gu F, Zhang LS. A conditionally replicating adenovirus expressing IL-24 acts synergistically with temozolomide to enhance apoptosis in melanoma cells in vitro. Oncol Lett. 2017;13(6):4185–4189. PMID: 28599419. doi:10.3892/ol.2017.6007.

18. Li Y, Zhao M, Guo C, Chu H, Li W, Chen X, Wang X, Li Y, Jia Y, Koussatidjoa S, et al. Intracellular mature IL-37 suppresses tumor metastasis via inhibiting Rac1 activation. Oncogene. 2018;37(8):1095–1106. PMID: 29106392. doi:10.1038/onc.2017.405.

19. Johnson DE, O'Keefe RA, Grandis JR. Targeting the IL-6/JAK/STAT3 signalling axis in cancer. Nat Rev Clin Oncol. 2018;15(4):234–248. PMID: 29405201. doi:10.1038/nrclinonc.2018.8.

20. Yanaihara N, Hirata Y, Yamaguchi N, Noguchi Y, Saito M, Nagata C, Takakura S, Yamada K, Okamoto A. Antitumor effects of interleukin-6 (IL-6)/interleukin-6 receptor (IL-6R) signaling pathway inhibition in clear cell carcinoma of the ovary. Mol Carcinog. 2016;55(5):832–841. PMID: 25856562. doi:10.1002/mc.22325.

21. Goumas FA, Holmer R, Egberts JH, Gontarewicz A, Heneweer C, Geisen U, Hauser C, Mende MM, Legler K, Rocken C, et al. Inhibition of IL-6 signaling significantly reduces primary tumor growth and recurrencies in orthotopic xenograft models of pancreatic cancer. Int J Cancer. 2015;137(5):1035–1046. PMID: 25604508. doi:10.1002/ijc.29445.

22. Hong D, Kurzrock R, Kim Y, Woessner R, Younes A, Nemunaitis J, Fowler N, Zhou T, Schmidt J, Jo M, et al. AZD9150, a next-generation antisense oligonucleotide inhibitor of STAT3 with early evidence of clinical activity in lymphoma and lung cancer. Sci Transl Med. 2015;7(314):314ra185. PMID: 26582900. doi:10.1126/scitranslmed.aac5272.

23. Bharadwaj U, Eckols TK, Xu X, Kasembeli MM, Chen Y, Adachi M, Song Y, Mo Q, Lai SY, Tweardy DJ. Small-molecule inhibition of STAT3 in radioresistant head and neck squamous cell carcinoma. Oncotarget. 2016;7(18):26307–26330. PMID: 27027445. doi:10.18632/oncotarget.8368.

24. Cheng Y, Wang X, Wang P, Li T, Hu F, Liu Q, Yang F, Wang J, Xu T, Han W. SUSD2 is frequently downregulated and functions as a tumor suppressor in RCC and lung cancer. Tumour Biol. 2016;37(7):9919–9930. PMID: 26815503. doi:10.1007/s13277-015-4734-y.

25. Wang W, Li T, Wang X, Yuan W, Cheng Y, Zhang H, Xu E, Zhang Y, Shi S, Ma D, et al. FAM19A4 is a novel cytokine ligand of formyl peptide receptor 1 (FPR1) and is able to promote the migration and phagocytosis of macrophages. Cell Mol Immunol. 2015;12(5):615–624. PMID: 25109685. doi:10.1038/cmi.2014.61.

26. Kim J, Kim J, Lee SH, Kepreotis SV, Yoo J, Chun JS, Hajjar RJ, Jeong D, Park WJ. Cytokine-like 1 regulates cardiac fibrosis via modulation of TGF-beta signaling. PLoS One. 2016;11(11):e0166480. PMID: 27835665. doi:10.1371/journal.pone.0166480.

27. Schmall A, Al-Tamari HM, Herold S, Kampschulte M, Weigert A, Wietelmann A, Vipotnik N, Grimminger F, Seeger W, Pullamsetti SS, et al. Macrophage and cancer cell cross-talk via CCR2 and CX3CR1 is a fundamental mechanism driving lung cancer. Am J Respir Crit Care Med. 2015;191(4):437–447. PMID: 25536148. doi:10.1164/rccm.201406-1137OC.

28. Li S, Lu J, Chen Y, Xiong N, Li L, Zhang J, Yang H, Wu C, Zeng H, Liu Y. MCP-1-induced ERK/GSK-3beta/Snail signaling facilitates the epithelial-mesenchymal transition and promotes the migration of MCF-7 human breast carcinoma cells. Cell Mol Immunol. 2017;14(7):621–630. PMID: 26996066. doi:10.1038/cmi.2015.106.

29. Kim JH, Kim SS, Han IH, Sim S, Mh A, Ryu JS. Proliferation of prostate stromal cell induced by benign prostatic hyperplasia epithelial cell stimulated with trichomonas vaginalis via crosstalk with mast cell. Prostate. 2016;76(15):1431–1444. PMID: 27325623. doi:10.1002/pros.23227.

30. Wang S, An W, Yao Y, Chen R, Zheng X, Yang W, Zhao Y, Hu X, Jiang E, Bie Y, et al. Interleukin 37 expression inhibits STAT3 to suppress the proliferation and invasion of human cervical cancer cells. J Cancer. 2015;6(10):962–969. PMID: 26316892. doi:10.7150/jca.12266.

31. Zhao D, Pan C, Sun J, Gilbert C, Drews-Elger K, Azzam DJ, Picon-Ruiz M, Kim M, Ullmer W, El-Ashry D, et al. VEGF drives cancer-initiating stem cells through VEGFR-2/Stat3 signaling to upregulate Myc and Sox2. Oncogene. 2015;34(24):3107–3119. PMID: 25151964. doi:10.1038/onc.2014.257.

32. Zhong Z, Wen Z, Darnell JJ. Stat3: a STAT family member activated by tyrosine phosphorylation in response to epidermal growth factor and interleukin-6. Science. 1994;264(5155):95–98. PMID: 8140422.

33. Fujimoto K, Ida H, Hirota Y, Ishigai M, Amano J, Tanaka Y. Intracellular dynamics and fate of a humanized anti-interleukin-6 receptor monoclonal antibody, tocilizumab. Mol Pharmacol. 2015;88(4):660–675. PMID: 26180046. doi:10.1124/mol.115.099184.

34. Kannappan R, Yadav VR, Aggarwal BB. Gamma-Tocotrienol but not gamma-tocopherol blocks STAT3 cell signaling pathway

through induction of protein-tyrosine phosphatase SHP-1 and sensitizes tumor cells to chemotherapeutic agents. J Biol Chem. 2016;291(32):16922. PMID: 27496963. doi:10.1074/jbc. A110.158378.

35. Slattery ML, Lundgreen A, Hines LM, Torres-Mejia G, Wolff RK, Stern MC, John EM. Genetic variation in the JAK/STAT/SOCS signaling pathway influences breast cancer-specific mortality through interaction with cigarette smoking and use of aspirin/ NSAIDs: the breast cancer health disparities study. Breast Cancer Res Treat. 2014;147(1):145–158. PMID: 25104439. doi:10.1007/ s10549-014-3071-y.

36. Lao M, Shi M, Zou Y, Huang M, Ye Y, Qiu Q, Xiao Y, Zeng S, Liang L, Yang X, et al. Protein inhibitor of activated STAT3 regulates migration, invasion, and activation of fibroblast-like synoviocytes in rheumatoid arthritis. J Immunol. 2016;196(2):596–606. PMID: 26667168. doi:10.4049/jimmunol.1403254.

37. Pan CM, Wang ML, Chiou SH, Chen HY, Wu CW. Oncostatin M suppresses metastasis of lung adenocarcinoma by inhibiting SLUG expression through coordination of STATs and PIASs signalings. Oncotarget. 2016;7(37):60395–60406. PMID: 27486982. doi:10.18632/oncotarget.10939.